

1 **Genomic and phenotypic characterization of *Burkholderia* isolates from the potable water**  
2 **system of the International Space Station**

3  
4 Aubrie O'Rourke<sup>1†</sup>, Michael D. Lee<sup>2†</sup>, William C. Nierman<sup>1</sup>, Chris L. Dupont<sup>1</sup>

5  
6 1: J. Craig Venter Institute, San Diego, CA USA

7 2: Exobiology Branch, NASA Ames Research Center, Mountain View, CA, USA

8  
9 † equal contribution

10

11 **Abstract**

12

13 The opportunistic pathogens *Burkholderia cepacia* and *Burkholderia contaminans*, both  
14 genomovars of the *Burkholderia cepacia* complex (BCC), are frequently cultured from the potable  
15 water system (PWS) of the International Space Station (ISS). Here, we sequenced the genomes  
16 and conducted phenotypic assays to characterize these *Burkholderia* isolates. All recovered  
17 isolates of the two species fall within monophyletic clades based on phylogenomic trees of  
18 conserved single-copy core genes. Within species, the ISS PWS strains all demonstrate greater  
19 than 99% average nucleotide identity (ANI), suggesting that they are of a highly similar genomic  
20 lineage and both individually may have stemmed from the two founding clonal strains before  
21 diverging into two unique sub strain populations. No evidence for horizontal gene transfer between  
22 the populations was observed. Differences between the recovered isolates can be observed at the  
23 pangenomic level, particularly within putative plasmids identified within the *B. cepacia* group.  
24 Phenotypically, the ISS-derived *B. cepacia* isolates generally exhibit a trend of lower rates and  
25 shorter duration of macrophage intracellularization compared to the selected terrestrial reference  
26 strain (though not significantly), and significantly lower rates of cellular lysis in 7 of the 19  
27 isolates. ISS-derived *B. contaminans* isolates displayed no difference in rates of macrophage  
28 intracellularization compared to the selected reference, though generally increased rates lysis, with  
29 2 of the 5 significantly increased at 12-hours post inoculation. We additionally find that ISS-  
30 isolated *B. contaminans* display hemolytic activity at 37°C not demonstrated by the terrestrial  
31 control, and greater antifungal capacity in the more recently collected isolates. Thankfully, the  
32 ISS-derived isolates generally exhibit 1-4 times greater sensitivity to common antibiotics used in  
33 their clinical treatments. Thus, despite their infection potential, therapeutic treatment should still  
34 have efficacy.

35

36 **Author Summary**

37

38 The International Space Station (ISS) is a unique built environment due to its isolation and  
39 recycling of air and water. Both microbes and astronauts inhabit the ISS, and the potential  
40 pathogenicity of the former is of great concern for the safety of the latter. The potable water  
41 dispenser (PWD) of the potable water system (PWS) on board the ISS was assembled in a  
42 cleanroom facility and then primed on Earth using an extensive process to ensure no gas bubbles  
43 existed within the lines that could lock the apparatus upon installation in orbit. The primed system  
44 sat dormant for 6 months before installation on the ISS. Microbial surveillance was conducted on  
45 the system after installation and the bacterial load was 85 CFU/mL, which exceeded the 50  
46 CFU/mL limits set for ISS potable water. Over a microbial surveillance spanning 4.5 years,

47 numerous strains of the potential pathogen *Burkholderia* have been isolated from the PWD. Here  
48 we sequenced and analyzed the genomes of these strains while also characterizing their potential  
49 pathogenicity. The genome analysis indicates it is likely that there were only two strains that were  
50 introduced on Earth that have subsequently undergone minimal diverging evolution. These strains  
51 retain pathogenicity, but remain susceptible to antibiotics, providing a potential therapeutic  
52 intervention in the event of infection.

53

## 54 **Introduction**

55

56 Microbial surveillance of the surfaces, air, and potable water system (PWS) of the  
57 International ISS has been implemented by National Aeronautics and Space Administration  
58 (NASA) to ensure crew health within this unique closed environment. These efforts, which use  
59 standard culturing techniques, have been conducted over twelve years and 22 missions and began  
60 shortly after the potable water dispenser (PWD) was launched on STS-126 in November of 2008  
61 . On-orbit operations using the PWD began in early 2009 and continues operations to this day. The  
62 organisms *Burkholderia cepacia* and *B. contaminans*, both genomovars of the *Burkholderia*  
63 *cepacia* complex (BCC), are frequently cultured from the PWD of the ISS. Our isolates were  
64 collected between January 6, 2010 during mission 22 to August 6, 2014 during mission 40 (Fig. 1,  
65 S1 Table). The PWS in combination with the PWD is a water recycling system that utilizes  
66 physical and chemical techniques to filter, decontaminate, and sterilize water used for drinking  
67 and food hydration [1–3]. *Burkholderia* spp. are known to withstand disinfection and sterilization  
68 procedures as they display a moderate to high-tolerance to stress such as UV-C radiation,  
69 antibiotics, and high heavy-metal concentrations [4].

70 *Burkholderia* spp., among other bacterial contaminants, are likely to have been introduced  
71 into the PWD during unit assembly on planet [1–3]. *Burkholderia* spp. probably sustained in the  
72 system due to the ability of this genera to survive long periods in distilled water [5,6]. This ability  
73 to survive in distilled water with minimal additives has made them problematic for healthcare, as  
74 hospital-acquired BCC infections can arise from contaminated disinfectants, anesthetic solutions,  
75 distilled water, and aqueous chlorhexidine solutions [4]. The ISS PWD uses flushes of 40ppm  
76 elemental iodine for decontamination, followed by iodine removal by a deiodination filter before  
77 astronaut use [1–3]. Some *Burkholderia* isolates have been found to be resistant to iodine and can  
78 even survive in iodine solutions [7] providing pre-observed phenotypes in this lineage capable of  
79 continued presence in the ISS PWD.

80 *Burkholderia* species are known to propagate in both nutrient-poor and -rich soil  
81 environments, in addition to within human host cells [8]. They are copiotrophs commonly isolated  
82 from soil, plant rhizospheres, and water [9], as well as from the sputum of cystic fibrosis patients  
83 with chronic infection [10]. BCC members pose a significant threat to individuals with cystic  
84 fibrosis (CF; accounting for 85% of all infections in CF patients [10]) and otherwise immune-  
85 compromised patients due to an exacerbation of pulmonary infections, which can lead to morbidity  
86 and mortality [11]. The antibiotic resistance and intracellular survival capabilities of BCC  
87 members make them unamenable to many therapeutics in susceptible patients are exposed to them  
88 [12]. The genomes of BCC organisms can mutate rapidly during infections or when subjected to  
89 high-stress conditions [13], the latter of which would be satisfied by the sequential iodine  
90 treatments of the PWD. The genus is known to have several mobile genetic elements (MGEs),  
91 which can promote the transfer and acquisition of virulence and antibiotic resistance genes; BCC  
92 organisms have genomic islands, such as the *B. cepacia* epidemic strain marker (BCESM),

93 containing genes linked to virulence and metabolism, quorum sensing, transcriptional regulation,  
94 fatty acid biosynthesis, and transposition [13]. Here we characterize genomic and phenotypic  
95 properties of 24 *Burkholderia* isolates derived from the ISS PWD.  
96

## 97 **Results**

98  
99 The PWD unit of the ISS was assembled in a cleanroom facility and then primed on Earth  
100 using an extensive process to ensure no gas bubbles existed within the lines that could lock the  
101 apparatus upon installation in orbit. The primed system sat dormant for 6 months before  
102 installation on the ISS [1,3]. Microbial surveillance was conducted on the system after installation  
103 and the bacterial load was 85 CFU/mL, which exceeded the 50 CFU/mL limits set for ISS potable  
104 water, leaving the sole source of water on the US module out-of-order [1]. In the meantime, the  
105 Russian system was used as a back-up. The US system was flushed with the biocide iodine (I<sub>2</sub>),  
106 first at what turned out to be a sub-inhibitory concentration of 4ppm, as subsequent measurements  
107 revealed an increase in the microbial load [1]. Further testing revealed that 40ppm was the  
108 necessary concentration of iodine flush to achieve the drinkable 50 CFU/mL bacterial load [1].  
109 Iodine flushes are still intermittently administered to the system after durations of PWS stagnation.  
110 Our focal *Burkholderia* species are known to survive not only in distilled water, but also in iodine  
111 solutions; therefore, these flushes may have reduced the overall microbial load of the PWS while  
112 inadvertently selecting for the *Burkholderia* species within the system. Here we characterized the  
113 *Burkholderia* species isolates obtained from the ISS PWS both genomically and phenotypically.

114 Twenty-four isolates collected over 4.5 years were chosen for sequencing. The genomes of  
115 24 ISS-PWD *Burkholderia* isolates (Fig. 1A) were sequenced and *de novo* assembled with SPAdes  
116 v3.12.0 ([14]; assembly summary information in S2 Table). The recovered genomes within each  
117 species were all found to have an ANI of greater than 99% with 95–99.9% alignment in all cases  
118 (fastANI v1.2; [15]). An estimated maximum-likelihood phylogenetic tree based on amino acid  
119 sequences of 203 single-copy genes specific to Betaproteobacteria was generated with GToTree  
120 v1.4.4 ([16]; Fig 1B). This placed 19 of the isolates within their own monophyletic clade within  
121 the *B. cepacia*, and 5 within their own monophyletic clade within the *B. contaminans* (Fig 1B).  
122 Single-nucleotide variant (SNV) trees (Parsnp v.1.2; [17]) generated for each group of isolates  
123 revealed no clear groupings based on time of isolation (Fig 1C). The *B. cepacia* were isolated over  
124 the entire sampling period, which *B. contaminans* were only isolated during 2013 and 2014.  
125

## 126 **Pangenomic Analysis**

127  
128 We first performed a pangenomic analysis of each species incorporating all assemblies  
129 available from NCBI (as accessed on 20-Aug-2019). Gene clusters (GCs) were identified with  
130 MCL clustering [18] as employed within anvi'o v5.5 [19]. Across the incorporated 155 *B. cepacia*  
131 genomes (136 reference from NCBI and 19 derived from the ISS PWS), the average gene count  
132 was 7,461 ± 479 (mean ± 1SD). The MCL clustering approach yielded the identification of 25,383  
133 total GCs: 2,589 with genes contributed by all (“core”; 10.2%); 8,249 with genes contributed by  
134 only single genomes (“singletons”; 32.5%); and 14,545 contributed by some mixture (“accessory”)  
135 (Fig 2A). A total of 25 *B. contaminans* genomes were incorporated (20 references from NCBI and  
136 5 ISS-isolates), with an average gene count of 7,580 ± 539. From these, a total of 13,645 GCs were  
137 generated: 3,534 core (25.9%); 3,436 singletons (25.2%); and 6,675 accessory GCs (49.0%; Fig  
138 2B). It should be noted the disparity between the number of identified core, singleton, and

139 accessory genes in *B. cepacia* vs those identified in *B. contaminans* at this point is not meant to  
140 convey anything about potential differences in gene-content diversity between the two species.  
141 The number of genomes available/incorporated for each and the breadth of phylogenetic diversity  
142 spanned by the incorporated genomes of the two groups both vary greatly.

143 We scanned for functional enrichment or depletion in the ISS-derived isolates as compared  
144 to the reference genomes based on normalized frequencies of presence/absence across the two  
145 groups (see Methods). It should be kept in mind that given the phylogenetic landscape of both ISS-  
146 derived groups – with each forming monophyletic clades within their respective species (Fig 1B)  
147 – the functional differences observed may be due to evolutionary divergence as a whole, rather  
148 than being due to their source of isolation (the ISS). Of the *B. contaminans* pangenome, this  
149 revealed no depleted functions in the ISS-derived isolates, and 8 functions enriched including those  
150 commonly associated with viruses and conjugative plasmids (Table 1; full results in S3 Table).

151  
152

**Table 1: ISS-derived *B. contaminans* enriched functions as compared to references.**

Annotation (NCBI PGAP)	Occurrence in ISS-isolates	Occurrence in Refs	Corrected p-value
Invasion protein lagB	5/5	0/20	0.09
Nucleoside 2-deoxyribosyltransferase	5/5	0/20	0.09
PH domain-containing protein	5/5	1/20	0.09
RepA replicase	5/5	1/20	0.09
Metallophosphatase family protein	5/5	1/20	0.09
Pilus assembly protein PilN	5/5	1/20	0.09
Prepilin type IV pili	5/5	1/20	0.09
Type IV secretion system protein VirB3	5/5	1/20	0.09

153

154 In contrasting the functional annotations of the 19 ISS-derived *B. cepacia* with the 136  
155 references, 265 functions were found to be enriched, with 98 found to be depleted (5 of each  
156 presented in Table 2; full results in S4 Table).

157

158 **Table 2: ISS-derived *B. cepacia* enriched/depleted functions as compared to references.**

Annotation (NCBI PGAP)	Occurrence in ISS-isolates	Occurrence in Refs	Corrected p-value
Toprim domain-containing protein	19/19	0/136	0.00
3-carboxyethylcatechol 2,3-dioxygenase	19/19	0/136	0.00
Metal transporter	19/19	1/136	0.00
Plasmid mobilization relaxosome MobC	19/19	1/136	0.00
Peptidase M4	19/19	3/136	0.00
Sugar transporter	0/19	133/136	0.00
LTA synthase family protein	0/19	132/136	0.00
Class II aldolase family protein	0/19	123/136	0.00
Nit6803 family nitriliase	0/19	111/136	0.00
MSMEG_0572 N starvation response	0/19	111/136	0.00

159

160 As noted above, the recovered genomes within each species were all found to have an ANI  
161 of greater than 99% with 95–99.9% alignment in all cases, and each form monophyletic clades in  
162 relation to other members of their respective species (Fig 1B). Pangenomic analyses of solely the  
163 ISS-derived isolates revealed highly conserved cores of GCs for both species, with greater than  
164 90% of the GCs having genes contributed from all genomes. For the 19 *B. cepacia* isolates, 7,688

165 total GCs were generated: 7,065 core (91.9%); only 20 singletons (0.26%); and 603 accessory GCs  
166 (7.8%; Fig 3, left side). Of the singleton GCs with functional annotations (5/20), most annotations  
167 were present in other GCs – meaning the sequences diverged enough to not cluster together, but  
168 were similar enough to be annotated the same way. The one exception was annotated by NCBI as  
169 an autotransporter domain-containing protein (from isolate s20, gene ID D7204\_40525). For the  
170 5 *B. contaminans* isolates, 7,778 GCs were generated: 7,509 core (96.5%); 163 singletons (2.1%);  
171 and 106 accessory GCs (1.4%). Of the 163 singleton GCs from *B. contaminans*, 46 had annotations  
172 associated with them. Twenty-eight of these annotations were found in other GCs, while 18 were  
173 only annotated in one genome. Interestingly, 17 of these 18 all came from the same isolate s47,  
174 which was the first *B. contaminans* isolate recovered from the ISS (Fig 1C); these functional  
175 annotations are presented in Table 3. All gene calls, sequences, and annotations are available in  
176 S5 Table.

177

178 **Table 3: *B. contaminans* singleton-GC functional annotations not identified in any other**  
179 **GCs.**

Annotation (NCBI PGAP)	Isolate	Gene ID
Nickel resistance protein	s47	D7S92_31485
Conjugal transfer protein TrbE	s47	D7S92_31155
Conjugal transfer protein TrbI	s47	D7S92_31155
DUF1259 domain-containing protein	s47	D7S92_31415
C-type cytochrome biogenesis protein CcsB (ccsB)	s47	D7S92_31465
Type IV secretion system family protein	s47	D7S92_31160
Toprim domain-containing protein	s47	D7S92_35590
P-type DNA transfer ATPase VirB11 (virB11)	s47	D7S92_31190
Replication initiator protein A	s47	D7S92_31330
Type II secretory pathway component PulF-like protein	s47	D7S92_31550
Chromate resistance protein	s47	D7S92_31420
Type IV secretion system protein VirD4	s47	D7S92_31125
Type IV secretion system protein VirB8	s47	D7S92_31175
Zinc metalloproteinase Mpr protein	s47	D7S92_31335
Zeta toxin family protein	s47	D7S92_31320
Nickel/cobalt efflux protein RcnA	s47	D7S92_31490
Conjugative relaxase	s47	D7S92_31130
Type IV secretion protein Rhs	s56	D7S91_34560

180

## 181 **Plasmid Analysis**

182

183 Putative plasmids were computationally identified in the ISS-derived isolates using  
184 plasmidSPAdes [20], which operates largely based on coverage. This process identified putative  
185 plasmid contigs from each of the 19 *B. cepacia* isolates and 2 of the 5 *B. contaminans* isolates (s47  
186 and s52; annotations and sequences for all can be found in S6 Table. Running a pangenomic  
187 analysis on the 19 *B. cepacia* putative plasmids generated a total of 916 GCs: 48 core (5.2%); 527  
188 singletons (57.5%); and 341 accessory GCs (37.2%; Fig 3, right side). Despite the high similarity  
189 between the ISS genomes as a whole, the majority of variability that does exist within their genetic  
190 complement (Fig 3, left side  $\approx$ 3-3:30 “o’clock”) appears to be sustained among the putative  
191 plasmids that were identified (Fig 4, right side). The 2 recovered putative plasmids from *B.*  
192 *contaminans* had little overlap based on GCs. With a total of 475 GCs, only 3 had genes



193 contributed from both genomes (0.6%), leaving the remaining 472 as singletons. Annotations from  
 194 NCBI's Clusters of Orthologous Genes (GOGs; [21]) of coding sequences from the putative  
 195 plasmids reveal elements typical of conjugative plasmids, such as DNA replication proteins  
 196 (DnaC), plasmid stabilization proteins (ParE), and Type IV secretion system components (T4SS;  
 197 Table 4). Additionally, in *B. cepacia* putative plasmids were identified a catechol 2,3-dioxygenase,  
 198 a contamination indicator as it is able to breakdown polycyclic aromatic hydrocarbons [22,23],  
 199 and lysophospholipase, an enzyme known to be used by ingested bacteria to avoid phagocytosis  
 200 by macrophage [24]. Despite containing this small conserved core, the larger plasmids in particular  
 201 contain multiple copies of genes with annotations such as bacteriophage DNA transposition  
 202 protein, AAA+ family ATPase (s9, s36, s39, s57), Virulence-associated protein-VagC (virulence  
 203 associated gene C; s16, s28, s35, s36, s39), and additional elements of the T4SS, VirB8 (S6 Table).  
 204 We additionally see transposases-related genes in the *B. cepacia* isolates with a mean copy number  
 205 per putative plasmid of  $17.57 \pm 5.7$  (mean  $\pm$  1 SD), and an integrase element with a mean copy  
 206 number of  $2.47 \pm 0.51$ , suggesting DNA rearrangements and duplications among the conjugative  
 207 plasmids of ISS *B. cepacia* may be a result of these mobile genetic elements.

208 As for *B. contaminans*, in addition to harboring elements of both the T4SS and Type II  
 209 secretion system (T2SS), the plasmids have a soluble lytic murein transglycosylase harboring a  
 210 putative invasion domain LysM at a mean copy number of  $3 \pm 2.8$ . The lytic transglycosylase,  
 211 LtgG, has recently reported for its role to control cell morphology and virulence in *Burkholderia*  
 212 *pseudomallei* [25]. Furthermore, we see each harboring a copy of the toxin component of the  
 213 MazEF toxin-antitoxin system suggesting these ISS *B. contaminans* isolates may be able to control  
 214 their transition to the dormant persister state [26]. Again, we see transposase-related genes with a  
 215 mean copy number of  $5 \pm 5.7$ .

**Table 4: COG functional annotations and copy numbers per putative plasmid for *B. cepacia* and *B. contaminans*.**

<b><i>B. cepacia</i> putative-plasmid annotations (19)</b>	
<b>Annotation (COG)</b>	<b>Mean copy # <math>\pm</math> 1 SD</b>
Plasmid stabilization system protein ParE	1 $\pm$ 0
Site-specific DNA-cytosine methylase	1 $\pm$ 0
Type IV secretory pathway, component VirB8	1 $\pm$ 0
Lysophospholipase	1.11 $\pm$ 0.5
Catechol 2,3-dioxygenase	1.84 $\pm$ 1.1
Arsenite efflux pump ArsB, ACR3 family	1.89 $\pm$ 1.1
Integrase	2.47 $\pm$ 0.5
DNA replication protein DnaC	3.05 $\pm$ 0.2
Cu/Ag efflux pump CusA	3.05 $\pm$ 3.4
DNA-binding transcriptional regulator, LysR family	3.11 $\pm$ 5.9
Transposase-related	17.11 $\pm$ 5.7
<b><i>B. contaminans</i> putative-plasmid annotations (2)</b>	
<b>Annotation (COG)</b>	<b>Mean copy # <math>\pm</math> 1 SD</b>
Cellulose biosynthesis protein BcsQ	1 $\pm$ 0
mRNA-degrading endonuclease, toxin component of the MazEF toxin-antitoxin module	1 $\pm$ 0
Tfp pilus assembly protein PilT, pilus retraction ATPase	1 $\pm$ 0
Type II secretory pathway component GspD/PulD (secretin)	1.5 $\pm$ 2.1
Type IV secretory pathway, component VirB8	1.5 $\pm$ 2.1

Type IV secretory pathway, VirB9 components	$2 \pm 1.4$
Chromosome segregation protein ParB	$2 \pm 0$
Chromate transport protein ChrA	$2 \pm 0$
DNA-binding protein H-NS	$2.5 \pm 0.7$
Soluble lytic murein transglycosylase	$3 \pm 2.8$
Transposase-related	$5 \pm 5.7$

216

217

## 218 **Macrophage Infection Assay**

218

219

220

221

222

223

224

225

226

227

228

229

230

231

232

233

234

235

The identification of putative virulence mechanisms within the conjugative plasmids of the ISS *Burkholderia* genomes led us to explore the ability for the ISS *B. cepacia* and *B. contaminans* isolates to invade and persist within macrophage in comparison to the terrestrial reference strains of *B. cepacia* ATCC25416 and *B. contaminans* J2956 in a cell culture. For reference, we have included two terrestrial strains from the same lineages (*B. cepacia* and *B. contaminans*), however must stress that these are not controls as they are different strains. Ideal controls would be terrestrial strains from within the monophyletic clades of ISS isolates. We used two metrics for this assessment: 1) the ability of the bacteria to invade macrophage cells and be retained intracellularly, which allows for the bacteria to replicate without lysosomal degradation in turn leading to chronic infections; and 2) the ability for the bacteria to cause macrophage cell lysis as assessed by the amount of lactate dehydrogenase (LDH) released by the cell. Such cell lysis in turn can trigger cytokine release and an inflammatory response. We present the cell counts for the intracellularized bacteria and LDH data for all ISS-derived isolates and *B. contaminans* J2956 and *B. cepacia* ATCC25416 reference strains. Macrophage cell lysis was quantified by the amount of LDH released in the cell culture media at six, eight, twelve and 24 hours post-inoculation (Fig 4). Bacteria which were internalized by macrophage were quantified and reported in colony forming units per milliliter (CFU/mL) measured at six and twelve hours post-inoculation (Fig 5).

236

237

238

239

240

241

242

243

244

245

246

At six and eight hours post infection, little LDH-release was observed for both the ISS-derived *B.cepacia* isolates and terrestrial control strain (Fig 4A). The *B. contaminans* ISS-derived isolates appear to be triggering cell lysis at a slightly greater rate than the terrestrial control, though with high variability across the experimental triplicates (Fig 4B) – likely due to higher rates of macrophage lysis observed in experiment two (S2 Fig). At six and eight hours, ISS isolates of *B. contaminans* in general display greater cellular lysis rates than those of the either the *B. cepacia* ATCC25416 or *B. contaminans* J2956 terrestrial control strains, though not significantly. At twelve hours post-infection, the lysis trend exhibited for each isolate exists but at twice the magnitude of LDH released at eight hours post infection (with s47 and s54 significantly greater than the terrestrial control J2956). Finally, at 24 hours post-infection, LDH release approaches that of triton-X, an example of full lysis (Fig 4).

247

248

249

250

251

At twelve hours post-infection it becomes apparent that the terrestrial strain of *B. cepacia* ATCC25416 is able to survive intracellularly within macrophage to a greater degree than any of the ISS isolates (Fig 5). It is this ability to persist within macrophage that tends to lead to chronic infection.

252

## 253 **Antifungal and Hemolysis Assay**

253

254

255

256

Non-ribosomal peptide synthetase (NRPS)-derived occidiofungin/burkholdine-like compounds are produced by *B. contaminans* via a gene cluster thought to have evolved to protect BCC bacteria from ecological niche predators such as amoeba and fungi [27]. Using antiSMASH

257 [28] we verified that each of the ISS isolates and the reference strain contain the occidiofungin and  
258 pyrrolnitrin gene cluster. The antifungal metabolite, occidiofungin, as well as pyrrolnitrin are  
259 known to also display hemolytic properties [29], which can break down heme in the hemoglobin  
260 of host bodies causing complications for the host.

261 Due to the identification of *B. contaminans* isolates harboring these two biosynthetic gene  
262 clusters within our collection, we assayed for the ability to inhibit growth of the *Aspergillus*  
263 *fumigatus* AF293 strain (Fig 6A) and cause hemolysis (Fig 6B). None of the *B. cepacia* isolates  
264 exhibited fungal inhibition or hemolysis, but each of the *B. contaminans* did to varying degrees.  
265 The terrestrial control reference strain (*B. contaminans* J2956) displayed the least amount of fungal  
266 inhibition (Fig 6A) and little to no hemolysis (Fig 6B), while isolate s47 displayed a similar ability  
267 to inhibit fungal growth but an added ability to lyse blood cells after 48 hours of growth. Though  
268 time of isolate-recovery does not necessarily indicate total time that isolate spent aboard the ISS,  
269 the isolates that display greater antifungal and hemolytic properties than s47 and the terrestrial  
270 control were collected at a later date (Fig 1A and 1C).

271

### 272 **Minimum Inhibition Concentration Assay**

273

274 ISS isolates and terrestrial reference control isolates were assayed for antibiotics commonly  
275 used in the clinical treatment of infections they are responsible for. These antibiotics included:  
276 cefotaxime, meropenem, and ceftazidime (cell wall synthesis inhibitors); ciprofloxacin (a  
277 topoisomerase inhibitor); cotrimethoprim (trimethoprim/sulfamethoxazole- a thymidine synthesis  
278 inhibitor); chloramphenicol (a 50S ribosomal subunit inhibitor); levofloxacin (a DNA synthesis  
279 inhibitor); and minocycline (a 30S ribosomal subunit inhibitor). Most isolates presented a  
280 minimum inhibitory concentration (MIC) within 1- to 4-fold that of the terrestrial control strains  
281 (*B. contaminans* J2956 and *B. cepacia* ATCC25416) for each antibiotic tested (Table 5). S33 was  
282 an exception as it appears to be more sensitive to co-trimethoprim. All isolates appeared to be  
283 moderately resistant to cefotaxime, yet susceptible to ceftazidime, also a 3<sup>rd</sup> generation  $\beta$ -lactam  
284 cephalosporin.

285



**Table 5: Minimum inhibitory concentration (MIC) values for all ISS-derived *Burkholderia* isolates and incorporated reference control strains.**

286

ug/mL	ceftazidime	cefotaxime	chloramphenicol	ciprofloxacin	cotrimethoprim	levofloxacin	minocycline	meropenem
<i>B. cepacia</i> ATCC25416	12	64	6	1	24	1	3	20
s9	8	64	7	2	17	6	10	32
s12	4	32	6	1	12	4	3	24
s16	4	32	8	1	20	4	5	10
s18	4	32	8	1	20	4	9	18
s20	8	32	8	1	24	4	9	18
s22	16	64	4	1	24	6	6	32
s23	4	64	4	2	24	6	6	16
s24	4	64	6	2	17	6	10	20
s25	8	64	6	1	24	6	6	24
s28	4	64	4	2	24	6	6	20
s31	8	64	4	1	24	4	4	24
s33	4	64	4	1	2	1	2	10
s35	8	64	6	1	48	3	8	32
s36	4	32	18	2	24	1	10	48
s37	8	64	5	2	32	2	6	32
s39	8	64	5	2	24	2	4	48
s40	4	64	24	1	4	2	10	64
s41	8	64	5	1	24	1	10	48
s57	8	64	8	1	16	1	2	6
<i>B. contaminans</i> J2956	8	64	8	1	8	1	2	4
s47	8	64	6	1	8	1	2	4
s52	8	64	8	1	6	1	2	4
s53	12	64	8	1	8	1	2	4
s54	12	64	8	1	6	1	2	4
s56	8	64	8	1	12	1	3	6

287

288

## 289 Biofilm Assay

290

291 The time of collection records show that the *Burkholderia* species are intermittently cultured  
 292 from the ISS PWD; there are numerous consecutive flights where *Burkholderia* could not be  
 293 cultivated from the PWD. One reason for this could be due to the proclivity for *Burkholderia*  
 294 species to form biofilms. This biofilm would be adapted over time to the pressure and flow  
 295 experienced during water removal from the system as needed for drinking or food hydration. We  
 296 observed the ability of the *B. cepacia* isolates to form biofilms to a slightly greater degree than  
 297 the *B. cepacia* terrestrial strains used for comparison (Fig 7A). We find that on a whole, *B.*  
 298 *contaminans* form biofilms more readily than *B. cepacia*, yet the ISS isolates of *B. contaminans*  
 299 have a diminishing ability to form biofilm in relation to the *B. contaminans* reference control  
 300 strain (Fig 7B).

301

## 302 Discussion

303

### 304 *Burkholderia* genomic analyses

305

306 The ISS-isolated *B. cepacia* and *B. contaminans* both formed monophyletic clades when  
 307 placed in a phylogenomic tree with currently available references (Fig 1B). When comparing the  
 308 ISS isolates among one another, they display very few single nucleotide polymorphisms (SNPs)  
 309 suggesting low genetic diversity among the respective ISS PWD strains. In a pangenomics

310 approach we identified core and accessory GCs for *B. cepacia* and *B. contaminans* and identified  
311 the functional annotations enriched and depleted in the ISS-derived isolates as compared to the  
312 incorporated references (Tables 1 and 2; S3 Table). There were a small number of functions strictly  
313 unique to the ISS isolates. *B. contaminans* isolates each contained two enriched functions  
314 annotated as an Invasion protein *iagB* and Nucleoside 2-deoxyribosyltransferase which were not  
315 identified in the 20 available terrestrial reference genomes queried. *IagB* is associated with  
316 *Salmonella enterica* subsp. *enterica* ser. Typhi invasion of HeLa cells [30]. *B. cepacia* isolates  
317 each contained two enriched functions annotated as a Toprim domain-containing protein and a 3-  
318 carboxyethylcatechol 2,3-dioxygenase that were not found in the 136 terrestrial reference control  
319 strains queried. Here, 3-carboxyethylcatechol 2,3-dioxygenase is involved in the breakdown of  
320 polycyclic aromatic hydrocarbons (PAHs) to be used as a carbon and energy source [31]. This  
321 pangenomic analysis indicates that the ISS isolates are certainly Earth-derived yet they have likely  
322 diverged due to the selective pressures imposed by the PWD.

323 One particular selective pressure that we know of is the iodine disinfection process used to  
324 maintain the PWD's bacterial load, which may have selected for these isolates and further  
325 streamlined their genomes to what they are now. Another explanation for their ability to survive  
326 these iodine shocks is their displayed propensity to form biofilms which will insulate members of  
327 the population from disinfection. Alternatives to iodine have been considered for future PWD  
328 microbial disinfection, such as the use of silver in the form of silver (I) fluoride [3,32]. The effect  
329 of silver treatment upon *B. cepacia* has been explored as a clinical alternative to antibiotics [33]  
330 and will likely reduce this microbial load. However, we find that the ISS *B. cepacia* isolates  
331 analyzed in this study all harbored a Cu/Ag efflux pump (*CusA*) at a mean copy number of  $3.05 \pm$   
332  $3.4$  on a conjugative plasmid (Table 4). This suggests that they will be able to share this ability to  
333 pump silver out from within their membrane with the subpopulations of the *B. cepacia* bacterial  
334 community that does not yet confer this resistance.

335 Similarly, we find a number of the identified enriched functions in our pangenomic analysis  
336 are commonly associated with mobile genetic elements that can be found on conjugative elements.  
337 A more in-depth plasmid analysis reveals that both species harbor elements of the Type IV  
338 secretion system (T4SS) on putative plasmids as well as an enrichment of transposase-related  
339 genes (S6 Table). Where, T4SSs are multi-subunit cell-envelope spanning structures consisting of  
340 a pilus and a secretion channel whereby DNA or protein is translocated outside of the cell to either  
341 a target cell or to the surrounding environment. T4SS mediates horizontal gene transfer, which  
342 contributes to genomic plasticity and the evolution of pathogens through the spread of antibiotic  
343 resistance or virulence genes [34]. The coverage-based plasmidSPAdes [20] approach identified  
344 putative plasmids in all 19 of the ISS *B. cepacia* isolates. A pangenomic view of these putative  
345 plasmids for *B. cepacia* revealed a conserved functional core of elements including the T4SS  
346 *VirD4* gene as well as a catechol 2,3-dioxygenase and lysophospholipase (Table 4). Putative  
347 plasmids were also identified in 2 of the 5 ISS *B. contaminans* isolates. These held similar  
348 functional annotations including lytic transglycosylase and the toxin component of the MazEF  
349 toxin-antitoxin system (Table 4).

350

### 351 ***Burkholderia cepacia* plasmid encoded features**

352

353 The ISS *B. cepacia* isolates all harbor at least one copy of lysophospholipase, this is an  
354 enzyme that frees fatty acids from lysophospholipids (LPLs) and in turn generates cytotoxic LPLs.  
355 As a result, LPLs are considered to be virulence factors of bacteria as they are found to help

356 bacteria escape phagosomes in host cells after a few rounds of intracellular multiplication [24].  
357 The cytotoxicity they generate allows the bacteria to rupture out of a macrophage or epithelial cell,  
358 and in addition, destroy lung surfactant and generate signal transducers such as  
359 lysophosphatidylcholine, which in turn can induce inflammation [24].

360 Catechol 2,3-dioxygenases (C23Os) found on the isolate putative plasmids are commonly  
361 used as water quality indicators [35]. C23Os degrade polycyclic aromatic hydrocarbons (PAHs)  
362 such as benzene, toluene, ethylbenzene, and xylenes, as well the degreaser and common  
363 groundwater contaminant trichloroethylene (TCE). Toluene has been identified among the organic  
364 compounds found in the humidity condensate samples from the US Space Shuttle Cabin [36]. The  
365 Shuttle did not use a water reclamation system, but the ISS does, as it reclaims water from urine  
366 and urine flush water, humidity condensate, personal hygiene water, and effluent from the crew  
367 health care systems. On a 1994 Shuttle mission, bags used to store urine samples for a life sciences  
368 experiment were giving off strong odors, and a post-flight assessment attributed this to the  
369 presence of volatile microbial metabolites which included 1,1,1-trichloroethane, and toluene [37].  
370 In addition, trichloroethene (TCE) was found in one of two samples processed from the galley  
371 cold-water ports on Mir-21 [38] in the range of 1.8-2.3 ug/L – the EPA has set a maximum  
372 contaminant level (MCL) of 5µg/L (5 ppb) in drinking water for TCE (U.S. Environmental  
373 Protection Agency 1985). Therefore, in the event that trace amounts of PAHs are present in the  
374 PWS, *Burkholderia* species maybe using C23Os to catabolize the compounds into usable carbon  
375 sources in order to facilitate their survival in the low-nutrient environment of the PWS of the ISS.

376 Furthermore the observation that transposase-related genes are present at a mean copy  
377 number of  $17.57 \pm 5.7$  per putative-plasmid, along with an integrase element with mean copy  
378 number of  $2.47 \pm 0.51$ , provides a possible beneficial mechanism when the population is under  
379 stress via promoting DNA rearrangement and duplications [36].

380

### 381 ***Burkholderia contaminans* plasmid encoded features**

382

383 The coverage-based approach of plasmidSPAdes [40] identified putative plasmids in 2 of  
384 the *B. contaminans* isolates (s47 and s52). Both possess annotated T4SS and T2SS components as  
385 well as a soluble lytic murein transglycosylase harboring a putative invasion domain LysM at a  
386 mean copy number of  $3 \pm 2.83$ . The lytic transglycosylase, LtgG, has recently reported for its role  
387 to control cell morphology in *Burkholderia pseudomallei* and its virulence in the BALB-C mouse  
388 model [25]. Both also harbor a copy of the toxin component of the MazEF toxin-antitoxin system  
389 suggesting the ability for these ISS *B. contaminans* isolates to control their transition to the  
390 dormant persister state. This is because toxin-antitoxin systems are known to contribute to cell  
391 dormancy by halting cellular machinery through use of the toxin that is counteracted by the  
392 antitoxin once the stressor is removed [26]. Again, we see duplicated transposase-related genes  
393 with a mean copy number of  $5 \pm 5.7$ .

394

### 395 **Phenotypic assessment of ISS *Burkholderia* species**

396

397 In order to test our hypothesis that these strains have the capacity to be virulent due to their  
398 plasmid gene content, we screened the ISS-derived *B. cepacia* and *B. contaminans* for the ability  
399 to invade and colonize macrophage. The *B. cepacia* isolates were found to invade macrophage by  
400 6 hours, with some (s33) being more effective colonizers than others. They appear to multiply,  
401 then escape from the macrophage by 12 hours post-inoculation, possibly using the plasmid-

402 encoded lysophospholipase mechanism to rupture the macrophage. Despite not contributing to a  
403 longer-term infection, the cytotoxic byproducts generated by lysophospholipase degradation of  
404 macrophage may play a physiological role in further stimulating the adhesion and differentiation  
405 of lymphoid cells macrophages and activation and recruitment of additional macrophage and T-  
406 lymphocytes, among other immune response mechanisms [24]. This is in contrast to the *B. cepacia*  
407 ATCC25416 terrestrial control strain, which has been noted for its ability to invade and carry out  
408 a long-term colonization of macrophage which can lend to the formation of long-term chronic  
409 infections [37]. We find that this strain displays the ability to remain intracellularized at 12-hours  
410 post-inoculation (Fig 5) yet remains able to lyse macrophage (Fig 4). Accordingly, the *B. cepacia*  
411 ATCC25416 reference strain contains additional virulence factors within its genome not found in  
412 the ISS isolates such as elements of the Type 6 secretion system (T6SS). *B. contaminans* isolates,  
413 on the other hand, seem to exhibit a decreased rate of cellular invasion and a more immediate cell  
414 lysis of macrophage. This follows suit with the hemolytic and antifungal capabilities they also  
415 display, which is not characteristic of the *B. cepacia* isolates. These ISS isolates appear slightly  
416 more virulent (as measured by LDH concentrations) than the incorporated *B. contaminans*  
417 terrestrial strain J2956, a pathogenic isolate from a sheep with mastitis. However, overall, the ISS  
418 *B. cepacia* and ISS *B. contaminans* isolates all appear to be less virulent to macrophage than the  
419 terrestrial reference *B. cepacia* strain.

420

## 421 **Methods**

422

### 423 **DNA isolation**

424

425 Bacterial isolates from the ISS PWD were obtained by filtering sample from both the  
426 ambient and hot water outlets of the potable water system through a microbial capture device  
427 (MCD) on the ISS by resident astronauts. The MCD filter was then placed on R2A agar and the  
428 plates were sent back to Earth for further isolation at JSC. Additionally, 1 liter of water was sent  
429 back in to Earth for further isolation at JSC on R2A agar. All isolates were cataloged and then  
430 stored at -80C in 15% glycerol until regrown on R2A agar slants and sent to JCVI. Upon arrival  
431 at JCVI all isolates were further plated on tryptic soy agar (TSA) and incubated overnight at 35°C,  
432 then inoculated into 4mls of tryptic soy broth (TSB). 2mls were stored with 15% glycerol as 1ml  
433 bacterial stocks and 2mls were centrifuged to form pellets with supernatant decanted then  
434 immediately frozen at -80C for future DNA extraction. DNA was extracted using a standard  
435 phenol/chloroform protocol. DNA was quantified using nanodrop and run on a gel to ensure high  
436 molecular weight samples were obtained.

437

### 438 **Genomic library preparation and sequencing**

439

440 400ng of high molecular weight bacterial in 13ul of 1X TE (10mM Tris pH 8.0, 1mM  
441 EDTA) was processed using the NEBNext Ultra II FS DNA Library Prep Kit for Illumina (New  
442 England Biolabs, Ipswich, MA) protocol at half the standard reaction volumes. To the 13ul DNA,  
443 3.5 ul of NEBNext Ultra II FS Reaction Buffer and 1ul of NEBNext Ultra II FS Enzyme was added  
444 in a PCR tube and then incubated in a thermocycler at 37°C for 10 minutes at 37°C for  
445 fragmentation to target size, the enzyme is then denatured by incubating the reaction at 65°C for  
446 30 minutes with lid set to 75°C. Next, adapter ligation is carried out on the 17.5 ul mixture of  
447 fragmented DNA by adding 15 ul of NEBNext Ultra II Ligation Master Mix, 0.5 ul of NEBNext

448 Ligation Enhancer, 1.25 ul of NEBNext Adapter for Illumina for a total volume of 34.25 ul. The  
449 34.25 ul adapter mixture is incubated at 20°C for 15 minutes a thermocycler with the heated lid  
450 off. This is followed by the addition of 1.5ul of USER Enzyme to the mixture, then incubation in  
451 the thermocycler at 37C for 15 minutes with heated lit set to 47C. In order to obtain 700-900 bp  
452 inserts, we used SPRIselect beads for a rightside clean-up of 0.25X, where the supernatant is  
453 retained for a left side clean up using a 0.25X bead clean up then eluted in 7.5 ul of 0.1X TE buffer.  
454 The fragmented, adapter ligated and size selected libraries were then amplified using 12.5 ul of  
455 NEBNext Ultra II Q5 Master Mix with 2.5 ul i7 index primer and 2.5 ul i5 Universal PCR primer  
456 for a total volume of 25 ul. The amplification was carried out at the following temperatures and  
457 times: initial denaturation at 98°C for 30 seconds, followed by 4 cycles of denaturation at 98°C for  
458 10 seconds and annealing/extension at 65°C for 75 seconds, and a final extension at 65°C for 5  
459 minutes. A total of 58 libraries were generated, quality controlled to find library size using the  
460 Agilent Bioanalyzer and high sensitivity DNA chip and double stranded DNA concentration was  
461 quantified using Qubit Fluorometric Quantitation. Libraries were normalized to achieve a total of  
462 700 pM of pooled library in 200 ul with an average library size of 750 bps. An average of 7 million,  
463 150 bp reads were obtained for the combined read 1 and read 2 of each library using Illumina's  
464 NextSeq 500 High Output Kit.

465

#### 466 **Genomic sequencing postprocessing**

467

468 For the 24 libraries, demultiplexing was carried out allowing 1 bp mismatch and adapters  
469 were trimmed. bcl2fastq2 Conversion Software v2.17 was used to check for adapters, if detected,  
470 base calls matching the adapter and beyond the match are masked or removed in the resultant  
471 FASTQ file. Sequence quality was assessed using the program FastQC [38]. Genomic DNA library  
472 forward and reverse reads were quality trimmed using trimmomatic v0.39 [39] with a sliding  
473 window of 5:20 and a minimum length of 100 base pairs. Libraries were de novo assembled using  
474 SPAdes v3.12.0 [14]. Assembly summaries are presented in S2 Table. Average nucleotide identity  
475 was calculated with fastANI v1.2 [15]. An estimated maximum-likelihood based with GToTree  
476 v1.4.4 [16] based on amino acid sequences of 203 single-copy genes specific to Betaproteobacteria  
477 using FastTree2 v2.1.10 [40]. Whole-genome assembly single-nucleotide variant (SNV) trees  
478 were generated with Parsnp v1.2 [17].

479 All pangenomic analyses were performed within anvi'o v5.5 [19], which uses MCL  
480 clustering [18]. Default settings were used other than setting the `--mcl-inflation` parameter to 7.

481

#### 482 **Functional enrichment/depletion analysis**

483

484 This was performed within anvi'o v5.5 (citation) utilizing the `anvi-get-enriched-  
485 functions-per-pan-group` program with default settings. The resulting table was filtered to include  
486 only those with a Benjamini-Hochberg corrected p-values of  $\leq 0.1$ .

487

#### 488 **Macrophage infection**

489

490 The infection assay aimed for a multiplicity of infection (MOI) of 5 ISS *B. cepacia* and *B.*  
491 *contaminans* cells for every one macrophage cell. Biological replicates of the experiment were  
492 conducted on three separate days to ensure a robust reproducibility in results. At time zero  
493 CFU/mL count was conducted for inoculum of each ISS isolate and was averaged for each



494 biological replicate experiment of the separate days (S1 Fig). These counts showed that our  
495 experimental MOI was in the range of MOI 5-11 with an average of MOI of 7 over the three  
496 replicated experiments. The bacteria were allowed to infect the macrophage cells for two hours  
497 before being washed away and replaced with fresh media containing 15ug/mL ceftazidime and  
498 1mg/ml amikacin to ensure clearance of extra cellular bacteria. At six, eight, twelve and 24 hours  
499 post-infection, the ISS treated sample supernatant and control supernatant from uninfected cells is  
500 collected and macrophage cells were removed by centrifugation at 300rpm for 2mins. The  
501 supernatant was then assessed for the presence of lactase dehydrogenase (LDH) using a  
502 Cytotoxicity Detection Kit (LDH) (Roche, Germany). The cell-free supernatant is incubated with  
503 the reaction mixture from the kit. LDH activity is determined using an enzymatic test. In the first  
504 step NAD<sup>+</sup> is reduced to NADH/H<sup>+</sup> by the LDH-catalyzed conversion of lactate to pyruvate. In  
505 the second step the catalyst (diaphorase) transfers H/H<sup>+</sup> from NADH/H<sup>+</sup> to the tetrazolium salt  
506 INT which is reduced to formazan. The enzyme reaction was stopped by the addition of 50 l/ well  
507 1N HCl (final concentration: 0.2 N HCl) after 10 minutes of incubation. The formazan dye  
508 absorbance was measured using the 490nm wavelength. We present the LDH data for all ISS  
509 strains and *B. contaminans* J2956 and *B. cepacia* ATCC25416 reference strains (S2 Fig, all LDH  
510 assay panels). Additionally, the macrophages were washed after removal of the supernatants at  
511 six, eight, twelve- and 24-hours post-infection to remove any dead extracellular bacterial cells,  
512 then lysed in order to enumerate the intracellular bacterial cells by plating and colony counting.

513

#### 514 **Aspergillus fumigatus screen**

515

516 JCVI -80°C freezer stocks were streaked onto TSA and incubated 48 hours at 37°C, single  
517 colonies were then inoculated into 3 mLs TSB and incubated overnight at 37°C with shaking at  
518 220rpm. *Aspergillus fumigatus* AF293 strain was maintained as glycerol stocks and grown at  
519 37°C. The fungus was incubated on Potato Dextrose Agar (PDA; Acumedia Manufactures Inc.  
520 Lansing, MI) at 37°C under the dark for 4 days. The fungal spores were collected with loops and  
521 suspended with 0.01% tween 80 sterilized water. The spore suspension was counted by  
522 hemocytometer and was inoculated to 10<sup>6</sup> spores per plate to PDA and TSA media, concurrently  
523 5 µl of a *Burkholderia* isolate was spotted in a quadrant of each of the agar types. The samples  
524 were incubated at 37°C and the zones of inhibition were recorded after 48hours.

525

#### 526 **Hemolysis assay**

527

528 JCVI -80°C freezer stocks were streaked onto TSA and incubated 48 hours at 37°C, single  
529 colonies were then inoculated into 3 mLs TSB and incubated overnight at 37°C with shaking at  
530 220 rpm. 5 µl of each *Burkholderia* isolate culture was spotted onto a petri plate (100mm x 15mm)  
531 containing TSA with 5% sheep's blood and incubated at 37°C for 48 hours.

532

#### 533 **MIC determination**

534

535 1xMICs of all antibiotics were determined using the National Committee for Clinical  
536 Laboratory Standards (NCCLS). In the MIC assay, 2ul of an antibiotic dilution series (beginning  
537 at 64ug/mL) was used to treat 100ul of OD<sub>600</sub>=0.001 culture (diluted from cells in exponential  
538 growth phase), then incubated without shaking for 18 hours before MIC determination. The MIC  
539 value is the lowest concentration at which bacterial growth is fully arrested.

540

## 541 **Biofilm assay**

542

543 JCVI -80°C freezer stocks were streaked onto TSA and incubated 48 hours at 35°C, single  
544 colonies were then inoculated into 3 mLs TSB and incubated overnight at 3°C with shaking at 220  
545 rpm. Cultures were diluted to an OD600 of 1, then diluted 1:100, each culture was then plated into  
546 one column of three 96 well polystyrene plates at 150 µl per well. The cultures were covered with  
547 adhesive film, then incubated at 35°C for 24, 48, and 72 hours. At each timepoint an entire 96 well  
548 plate having 11 cultures and control culture were stain using crystal violet. This process includes  
549 removing the cultured media from each well by inverting the plate and giving it 3-5 abrupt shakes  
550 into a waste container, then rinsing the wells lightly with water. This is followed by the addition  
551 of 150 µl of crystal violet into each well, the crystal violet is incubated in the well to adhere to any  
552 remaining biofilm for exactly 15 minutes, then the plate is carefully inverted and given 3-5 abrupt  
553 shakes into a crystal violet waste container. The plate is carefully rinsed with water and then laid  
554 upside down to dry. Once each of the 3 time points have been processed, the crystal violet is  
555 resolubilized for each timepoint plate using 100% EtOH by pipette mixing, then transferred to a  
556 new plate and covered to avoid evaporation. The resolubilized crystal violet strain is then placed  
557 in a plate reader to obtain an absorbance at 590 nm.

558

## 559 **Data availability**

560 The genomes reported in this paper can be found under bioproject: PRJNA493516.

561

## 562 **Acknowledgments**

563 AOR was funded by NASA Space Biology under grant 80NSSC17K0035.

564 MDL was funded by NASA Space Biology under grant NNH16ZTT001N-MOBE.

565 CLD was funded by the NASA Astrobiology Institute Alternative Earth's.

566

567

## 568 **Author Contributions**

569 Experiments were conducted by AOR. Bioinformatic analyses were conducted by AOR, MDL,  
570 and CLD. The manuscript was written by AOR and ML and CLD. Experiments were devised in  
571 collaborative effort by AOR, WCN, and CLD.

572

## 573 **References**

- 574 1. Toon K, Lovell R. International Space Station United States On-orbit Segment Potable  
575 Water Dispenser On-orbit Functionality vs. Design. 2012. doi:10.2514/6.2010-6250
- 576 2. Shaw LA, Barrera JL. International Space Station USOS Potable Water Dispenser  
577 Development. 2010;
- 578 3. Maryatt BW. Lessons Learned for the International Space Station Potable Water  
579 Dispenser. 2018;
- 580 4. Ryan MP, Adley CC. The antibiotic susceptibility of water-based bacteria *Ralstonia*  
581 *pickettii* and *Ralstonia insidiosa*. *J Med Microbiol.* 2013;62: 1025–1031.  
582 doi:10.1099/jmm.0.054759-0
- 583 5. Zurita J, Mejia L, Zapata S, Trueba G, Vargas AC, Aguirre S, et al. Healthcare-associated  
584 respiratory tract infection and colonization in an intensive care unit caused by  
585 *Burkholderia cepacia* isolated in mouthwash. *Int J Infect Dis.* International Society for

- 586 Infectious Diseases; 2014;29: e96–e99. doi:10.1016/j.ijid.2014.07.016
- 587 6. Ali M. Burkholderia Cepacia in Pharmaceutical Industries. Int J Vaccines Vaccin. 2016;3:  
588 2–4. doi:10.15406/ijvv.2016.03.00064
- 589 7. Panlilio AL, Beck-Sague CM, Siegel JD, Anderson RL, Yetts SY, Clark NC, et al.  
590 Infections and pseudoinfections due to povidone-iodine solution contaminated with  
591 pseudomonas cepacia. Clin Infect Dis. 1992; doi:10.1093/clinids/14.5.1078
- 592 8. Valvano MA, Keith KE, Cardona ST. Survival and persistence of opportunistic  
593 Burkholderia species in host cells. Current Opinion in Microbiology. 2005. pp. 99–105.  
594 doi:10.1016/j.mib.2004.12.002
- 595 9. Miller SCM, LiPuma JJ, Parke JL. Culture-based and non-growth-dependent detection of  
596 the Burkholderia cepacia complex in soil environments. Appl Environ Microbiol.  
597 2002;68: 3750–3758. doi:10.1128/AEM.68.8.3750-3758.2002
- 598 10. Tegos GP, Haynes MK, Schweizer HP. Dissecting novel virulent determinants in the  
599 Burkholderia cepacia complex. Virulence. 2012;3: 2. doi:10.4161/viru.19844
- 600 11. Ganesan S, Sajjan US. Host Evasion by *Burkholderia cenocepacia*. Front Cell Infect  
601 Microbiol. 2011;1: 25. doi:10.3389/fcimb.2011.00025
- 602 12. Valvano MA. Intracellular survival of burkholderia cepacia complex in phagocytic cells.  
603 Canadian Journal of Microbiology. 2015. doi:10.1139/cjm-2015-0316
- 604 13. Baldwin A, Sokol PA, Parkhill J, Mahenthiralingam E. The Burkholderia cepacia  
605 Epidemic Strain Marker Is Part of A Novel Genomic Island Encoding Both Virulence and  
606 Metabolism-Associated Genes in Burkholderia cenocepacia. Infect Immun. 2004;72:  
607 1537–1547. doi:10.1128/IAI.72.3.1537-1547.2004
- 608 14. Bankevich A, Nurk S, Antipov D, Gurevich AA, Dvorkin M, Kulikov AS, et al. SPAdes:  
609 A new genome assembly algorithm and its applications to single-cell sequencing. J  
610 Comput Biol. 2012; doi:10.1089/cmb.2012.0021
- 611 15. Jain C, Rodriguez-R LM, Phillippy AM, Konstantinidis KT, Aluru S. High throughput  
612 ANI analysis of 90K prokaryotic genomes reveals clear species boundaries. Nat Commun.  
613 2018; doi:10.1038/s41467-018-07641-9
- 614 16. Lee MD. GToTree: a user-friendly workflow for phylogenomics. Bioinformatics. 2019;  
615 doi:10.1093/bioinformatics/btz188
- 616 17. Treangen TJ, Ondov BD, Koren S, Phillippy AM. The harvest suite for rapid core-genome  
617 alignment and visualization of thousands of intraspecific microbial genomes. Genome  
618 Biol. 2014; doi:10.1186/s13059-014-0524-x
- 619 18. Van Dongen S, Abreu-Goodger C. Using MCL to extract clusters from networks.  
620 Methods Mol Biol. 2012; doi:10.1007/978-1-61779-361-5\_15
- 621 19. Eren AM, Esen ÖC, Sogin ML, Quince C, Delmont TO, Morrison HG, et al. Anvi'o: an  
622 advanced analysis and visualization platform for 'omics data. PeerJ. 2015;  
623 doi:10.7717/peerj.1319
- 624 20. Antipov D, Hartwick N, Shen M, Raiko M, Lapidus A, Pevzner PA. PlasmidSPAdes:  
625 Assembling plasmids from whole genome sequencing data. Bioinformatics. 2016;  
626 doi:10.1093/bioinformatics/btw493
- 627 21. Galperin MY, Makarova KS, Wolf YI, Koonin E V. Expanded Microbial genome  
628 coverage and improved protein family annotation in the COG database. Nucleic Acids  
629 Res. 2015; doi:10.1093/nar/gku1223
- 630 22. Táncsics A, Szabó I, Baka E, Szoboszlay S, Kukolya J, Kriszt B, et al. Investigation of  
631 catechol 2,3-dioxygenase and 16S rRNA gene diversity in hypoxic, petroleum

- 632 hydrocarbon contaminated groundwater. *Syst Appl Microbiol*. 2010;  
633 doi:10.1016/j.syapm.2010.08.005
- 634 23. Wikström P, Wiklund A, Andersson AC, Forsman M. DNA recovery and PCR  
635 quantification of catechol 2,3-dioxygenase genes from different soil types. *J Biotechnol*.  
636 1996; doi:10.1016/S0168-1656(96)01635-5
- 637 24. Flieger A, Gong S, Faigle M, Stevanovic S, Cianciotto NP, Neumeister B. Novel  
638 lysophospholipase a secreted by *Legionella pneumophila*. *J Bacteriol*. 2001;  
639 doi:10.1128/JB.183.6.2121-2124.2001
- 640 25. Jenkins CH, Wallis R, Allcock N, Barnes KB, Richards MI, Auty JM, et al. The lytic  
641 transglycosylase, LtgG, controls cell morphology and virulence in *Burkholderia*  
642 *pseudomallei*. *Sci Rep*. 2019; doi:10.1038/s41598-019-47483-z
- 643 26. Cho J, Carr AN, Whitworth L, Johnson B, Wilson KS. MazEF toxin-antitoxin proteins  
644 alter *Escherichia coli* cell morphology and infrastructure during persister formation and  
645 regrowth. *Microbiol (United Kingdom)*. 2017; doi:10.1099/mic.0.000436
- 646 27. Thomson ELS, Dennis JJ. A *Burkholderia cepacia* complex non-ribosomal peptide-  
647 synthesized toxin is hemolytic and required for full virulence. *Virulence*. 2012;  
648 doi:10.4161/viru.19355
- 649 28. Medema MH, Blin K, Cimermancic P, De Jager V, Zakrzewski P, Fischbach MA, et al.  
650 AntiSMASH: Rapid identification, annotation and analysis of secondary metabolite  
651 biosynthesis gene clusters in bacterial and fungal genome sequences. *Nucleic Acids Res*.  
652 2011; doi:10.1093/nar/gkr466
- 653 29. Nunvar J, Kalferstova L, Bloodworth RAM, Kolar M, Degrossi J, Lubovich S, et al.  
654 Understanding the pathogenicity of *Burkholderia contaminans*, an emerging pathogen in  
655 cystic fibrosis. *PLoS One*. 2016;11. doi:10.1371/journal.pone.0160975
- 656 30. Miras I, Hermant D, Arricau N, Popoff MY. Nucleotide sequence of *iagA* and *iagB* genes  
657 involved in invasion of HeLa cells by *Salmonella enterica* subsp. *enterica* ser. Typhi. *Res*  
658 *Microbiol*. 1995; doi:10.1016/0923-2508(96)80267-1
- 659 31. Soil RD, Garrido-sanz D, Redondo-nieto M. Metagenomic Insights into the Bacterial  
660 Functions of a Diesel-Degrading Consortium for the.
- 661 32. Toon K, Lovell R. International Space Station United States On-orbit Segment Potable  
662 Water Dispenser On-orbit Functionality vs. Design. 2012; 1–11. doi:10.2514/6.2010-6250
- 663 33. Pompilio A, Geminiani C, Bosco D, Rana R, Aceto A, Bucciarelli T, et al.  
664 Electrochemically synthesized silver nanoparticles are active against planktonic and  
665 biofilm cells of *Pseudomonas aeruginosa* and other cystic fibrosis-associated bacterial  
666 pathogens. *Front Microbiol*. 2018; doi:10.3389/fmicb.2018.01349
- 667 34. Juhas M, Crook DW, Hood DW. Type IV secretion systems: Tools of bacterial horizontal  
668 gene transfer and virulence. *Cell Microbiol*. 2008;10: 2377–2386. doi:10.1111/j.1462-  
669 5822.2008.01187.x
- 670 35. Kukor JJ, Olsen RH. Catechol 2,3-dioxygenases functional in oxygen-limited (hypoxic)  
671 environments. *Appl Environ Microbiol*. 1996;
- 672 36. Casacuberta E, González J. The impact of transposable elements in environmental  
673 adaptation. *Molecular Ecology*. 2013. doi:10.1111/mec.12170
- 674 37. Gronow S, Noah C, Blumenthal A, Lindner B, Brade H. Construction of a deep-rough  
675 mutant of *Burkholderia cepacia* ATCC 25416 and characterization of its chemical and  
676 biological properties. *J Biol Chem*. 2003; doi:10.1074/jbc.M206942200
- 677 38. Andrews S. FASTQC A Quality Control tool for High Throughput Sequence Data.

- 678 Babraham Inst. 2015;  
 679 39. Bolger AM, Lohse M, Usadel B. Trimmomatic: A flexible trimmer for Illumina sequence  
 680 data. *Bioinformatics*. 2014; doi:10.1093/bioinformatics/btu170  
 681 40. Price MN, Dehal PS, Arkin AP. FastTree 2 - Approximately maximum-likelihood trees  
 682 for large alignments. *PLoS One*. 2010;5. doi:10.1371/journal.pone.0009490  
 683

684 **Figures**

685

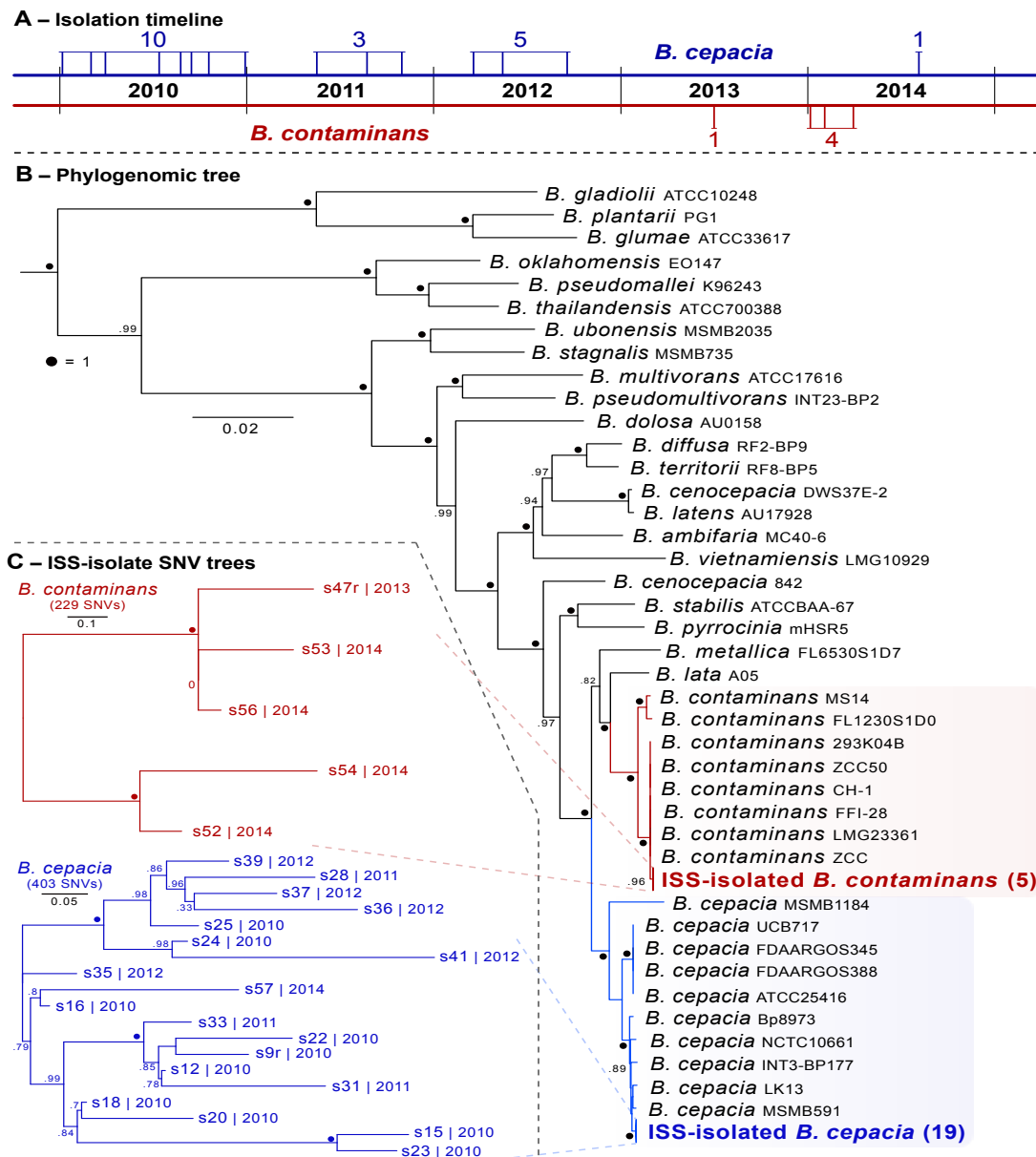


**Fig 1: Isolate phylogenetics.** (A) Isolation timeline (dates with multiple isolates are represented by a single line). (B) Estimated maximum-likelihood phylogenomic tree based on aligned and concatenated amino acid sequences of 203 single-copy genes designed for targeting Betaproteobacteria – rooted with *Ralstonia pickettii* 12J (GCF\_000020205.1). Numbers in parentheses indicate number of isolates in that clade. (C) ISS-derived isolate SNV trees for each *Burkholderia* species. Numbers following the identifiers are the year of isolation for that isolate.



686

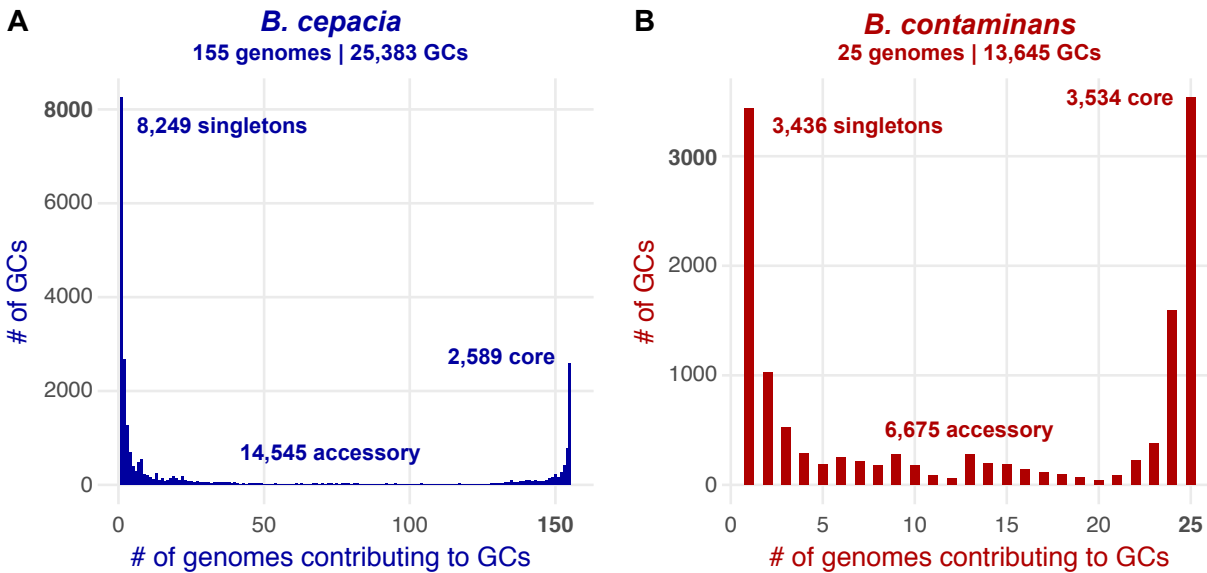


Fig 2: Gene-cluster distributions for (A) *B. cepacia* and (B) *B. contaminans*.

687

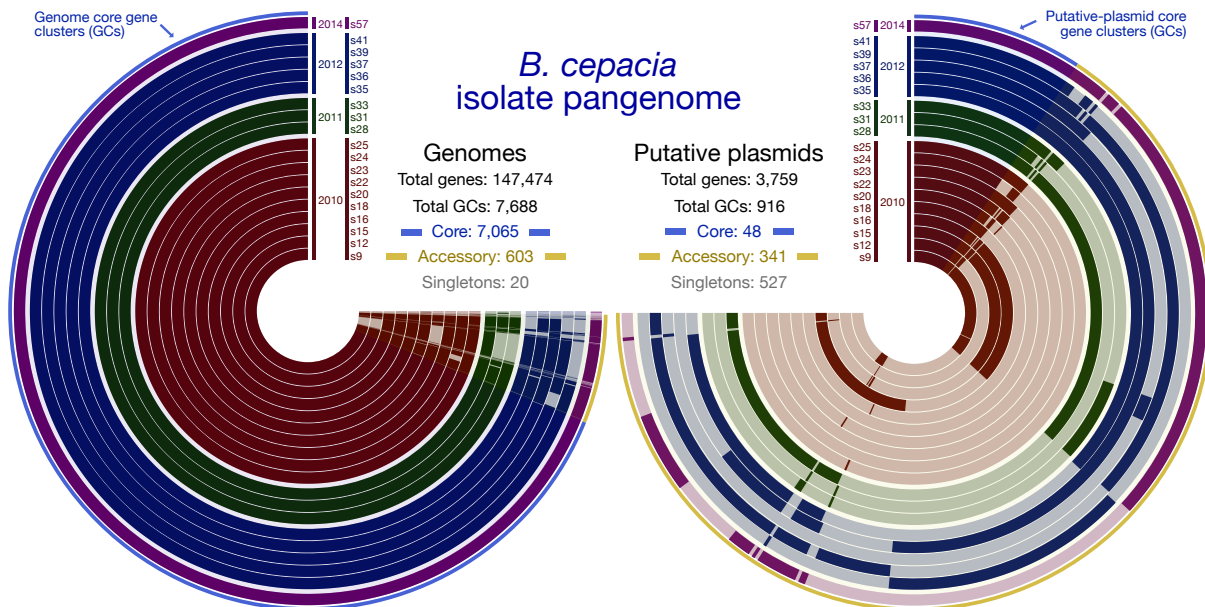


Fig 3: Pangenomics visualizations of the 19 ISS *B. cepacia* isolate genome assemblies (left) and identified putative plasmids (right). Each concentric circle radiating out from the center represents an isolate, identified at the top of each next to the year they were isolated. Wrapping around the circles are the generated gene clusters (GCs), where a solid mark for an isolate at a given GC indicates that particular isolate contributed a gene to that gene cluster, and the absence of a solid color indicates that isolate did not contribute a gene to that gene cluster. The very outer layer of each is a blue and yellow line. The blue line highlights core gene clusters. The yellow line highlights accessory GCs. The putative-plasmid pangenome on the right does not include singletons in the visualization.

688

689

690

691

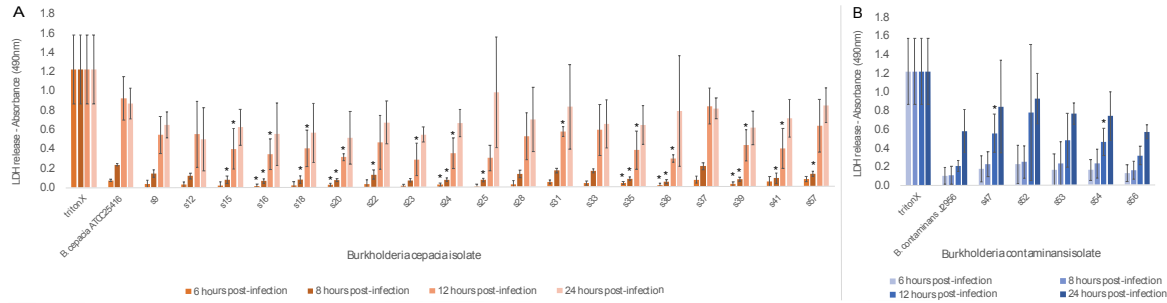


**Fig 4: Lactase dehydrogenase (LDH) release from macrophage 8 hours, 12 hours and 24 hours post exposure to Burkholderia isolates (A) *B.cepacia* and (B) *B. contaminans* along with terrestrial reference strains. Increase absorbance correlates to increase LDH release from macrophage. Symbols indicate significant difference from corresponding terrestrial reference at 0.05 threshold. “TritonX” exemplifies complete lysis.**

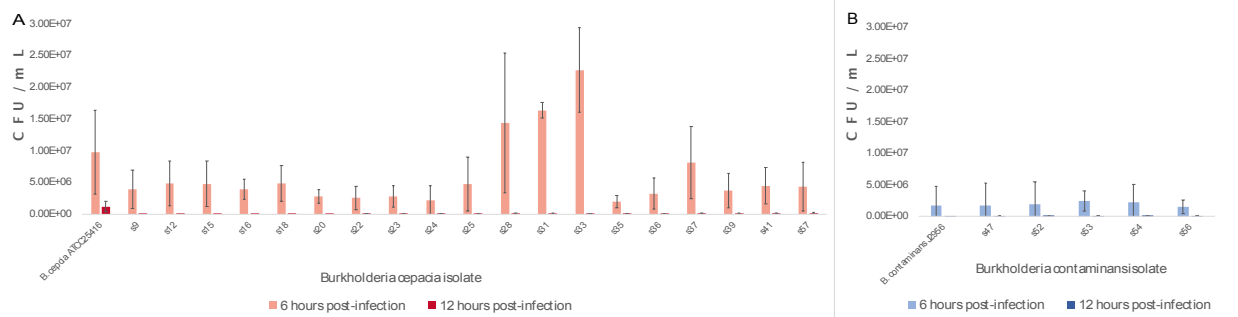


**Fig 5: Colony forming unit per milliliter (CFU/ml) counts of Burkholderia isolates (A) *B.cepacia* and (B) *B. contaminans* and terrestrial reference strain intracellularized by J774A.1 mouse macrophage.**

692  
693  
694  
695  
696  
697  
698  
699  
700  
701  
702  
703

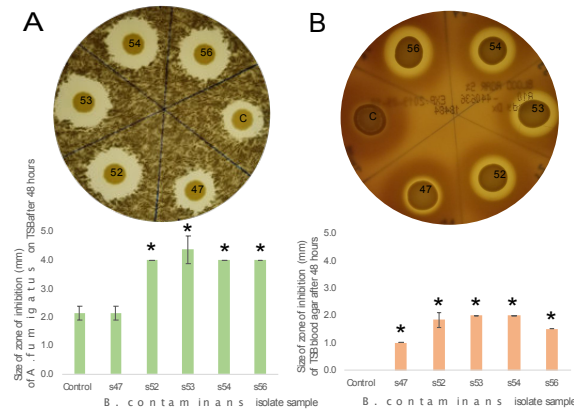
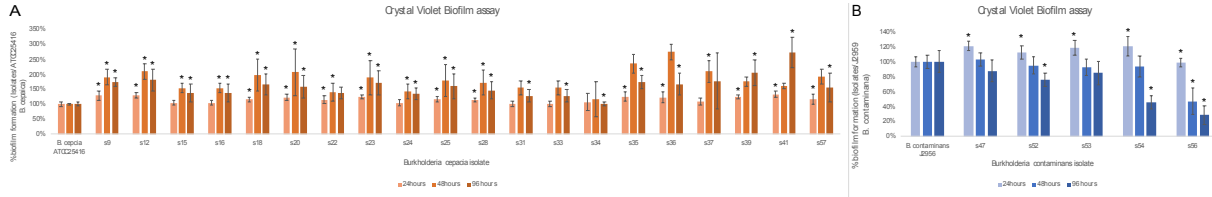


**Fig 6: ISS *B. contaminans* – known to produce the antifungal occidiofungin – (A) zones of inhibition formed on *Aspergillus fumigatus*. (B) Zones of inhibition presented by ISS *B. contaminans* on TSB plates with 5% sheep’s blood.**

704  
705  
706  
707  
708  
709  
710



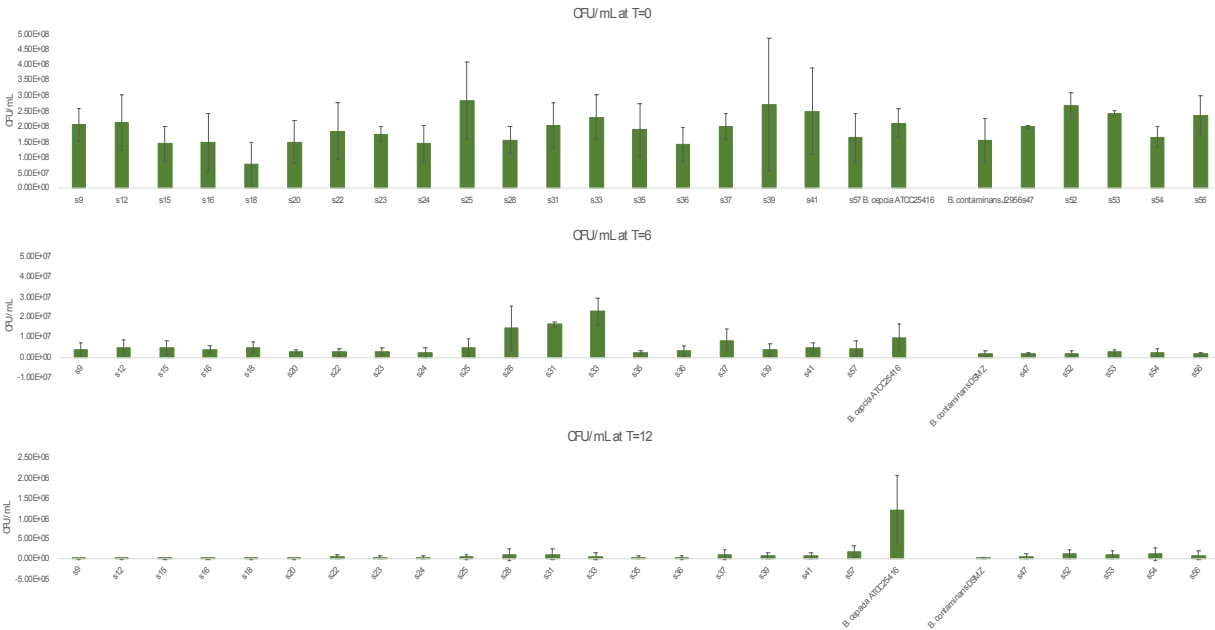
711

**Fig 7: % biofilm formation** for all ISS *Burkholderia* isolates **(A) *B.cepacia*** and **(B) *B. contaminans*** in relation to the respective terrestrial control strain.

712

713

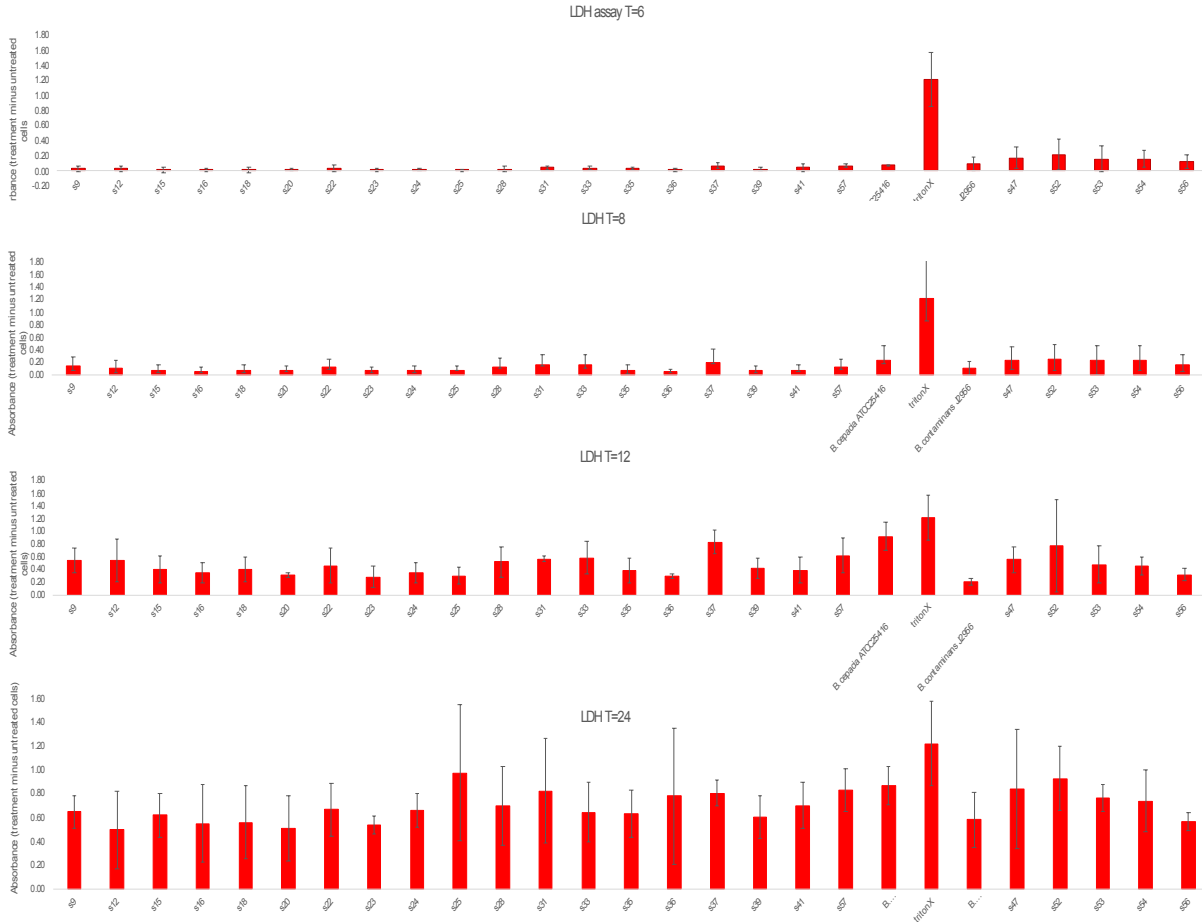
### Supplemental Figures



714

715

**Supplemental Figure1: Macrophage experiment CFU/mL time course data.**



716  
717 **S2 Fig. Macrophage experiment LDH time course data.**  
718

719 **Supplemental Tables**

- 720  
721 **S1 Table: Dates of isolation and sample number to NASA identifier.**  
722 **S2 Table: Spades Assembly data**  
723 **S3 Table: *B. contaminans* functional enrichments**  
724 **S4 Table: *B. cepacia* functional enrichments**  
725 **S5 Table: ISS isolate only pangenome with annotations and sequences**  
726 **S6 Table: ISS isolate only plasmid pangenome with annotations and sequences**  
727  
728  
729  
730  
731